PHYSICAL REVIEW B VOLUME 23, NUMBER 7 1 APRIL 1981

Calculation of finite-size effects and extraction of surface characteristics

D. J. E. Callaway and M. Schick
Department of Physics, University of Washington, Seattle, Washington 98195
(Received 17 September 1980)

We demonstrate a procedure for extracting surface characteristics of a substrate from thermodynamic information obtained from systems adsorbed upon that substrate. To do this we first employ renormalization-group approximations to calculate the specific heat of lattice-gas systems of various finite sizes. Results for the square lattice are in good agreement with exact results of Ferdinand and Fisher. Similar results for a honeycomb lattice are also presented. We then model the substrate as an assembly of platelets with a distribution of sizes. The specific heat from this model substrate is then compared to experimental data to obtain the parameters of the size distribution. Employing this procedure with data taken on the system of helium adsorbed on krypton-plated graphite, we determine that the mean platelet size is 140 Å with a root-mean-square deviation of 106 Å. We further conclude that about 50% of the adsorbed helium does not participate in the order-disorder transition.

I. INTRODUCTION

There have been several experimental attempts to determine the critical exponents of order-disorder transitions in adsorbed systems.[1–5] In each of these experiments the effects of finite sample size have been manifest and have complicated the extraction of the critical exponents. We show that these same effects can be turned to advantage to yield useful characteristics of the adsorbing substrate. Our analysis relies upon a model of a substrate comprised of a distribution $\rho(N)$ of subsystems each containing N atoms and a renormalization-group method of calculating the thermodynamic functions of such subsystems. The utility of the method is demonstrated on the system of helium adsorbed on krypton-plated graphite.[4]

Several effects of finite sample size and substrate heterogeneity on thermodynamic properties have been discussed previously. Probably the most important effect in the vicinity of a phase transition is the rounding of all singularities and the loss of all divergences due to the fact that the system comprises only a finite number of particles.[6,7] The evolution of the singularities as the number of particles increases without limit is predicted by finite-size scaling.[8] The nature of the boundary condition of the finite sample affects both the location and magnitude of maxima in the sample's thermodynamic responses such as its specific heat. Shifts in the temperature of the maximum from the bulk transition temperature are not of interest to us because, in the absence of a perfect substrate as referent, these shifts have not been measured. Contributions to the magnitude arise from the effect of the different number or strength of the interactions which particles at the edges feel relative to those in the interior.[9] This contribution clearly scales as the perimeter of the system and hence is generally smaller than that which scales as the area by a "surface-to-volume" factor of ξ/L, where ξ is the correlation length of the two-dimensional system. In the temperature regime in which finite size effects are important, $\xi \sim L$ so that the contributions are generally of the same magnitude. In Ising transitions, however,[6] the perimeter contribution is reduced by $\xi/(L \ln\xi)$ which never exceeds $1/\ln L$. We shall assume that for the sizes of interest, this factor is sufficiently small that the contribution can be ignored, an assumption which can be checked *a posteriori*. In particular, we employ periodic boundary conditions which, by treating the particles of the perimeter identically to those in the interior, guarantees the absence of a contribution which scales as the perimeter.

We ignore effects produced by a variation in the energies of adsorption[10–12] and thus in the chemical potential μ. They are negligible when measurements are taken in a region in which $T_c(\mu)$ is a maximum, as in the case of interest to us, for there T_c is independent of μ. The new component of our analysis is to include the effects of a distribution of finite-size systems which changes the shape of the specific-heat signal from that obtained from a single domain of finite size.

In the next section we present our renormalization-group procedure for calculating the thermodynamic properties of finite-size systems. We apply the method to an order-disorder transition of the square lattice and find very good agreement with exact results of Ferdinand and Fisher.[6] We also apply it to order-disorder transitions on the honeycomb lattice gas, a model for the system of helium on krypton-

 ©1981 The American Physical Society

plated graphite. In the final section, these results are combined with our model substrate and compared to the experimental results of Tejwani *et al.*[4] This comparison yields a mean size of a uniform region of krypton-plated graphite foam to be 140 Å with a standard deviation of 106 Å. Perhaps our most surprising result is that some 50% of the adsorbed helium atoms do not take part in the transition.

II. CALCULATION OF FINITE-SIZE EFFECTS

The renormalization-group transformation[13] maps a Hamiltonian $H_N(K,\{S\})$ governing N spins S and characterized by the couplings K to a Hamiltonian of the same form $H_{N'}(K',\{S'\})$ governing $N'<N$ spins S' and characterized by a set of couplings K'. The mapping can be written

$$\exp[\mathcal{H}_{N'}(K',\{S'\})+Ng(K,N)] = \sum_{\{S\}} P(\{S\},\{S'\})\exp\mathcal{H}_N(K,\{S\}) , \quad (2.1)$$

where P is a projection operator subject to

$$\sum_{\{S'\}} P(\{S\},\{S'\}) = 1 \quad (2.2)$$

and is otherwise arbitrary except for constraints of symmetry. The renormalized couplings K' are functions of the couplings K

$$K' = K'(K) . \quad (2.3)$$

It follows from Eq. (2.1) and the definition of the free energy per spin f that

$$f(K,N) = g(K,N)+b^{-d}f(K',b^{-d}N) , \quad (2.4)$$

where $N'=b^{-d}N$ with d the dimensionality of the system. With the aid of Eq. (2.3) this equation can be iterated

$$f(K,N) = \sum_{n=0}^{m} \frac{g(K^{(n)},b^{-nd}N)}{b^{nd}} + \frac{f(K^{(m+1)},b^{-(m+1)d}N)}{b^{(m+1)d}} , \quad (2.5)$$

where $K^{(n)}$ is the nth iterate and $K=K^{(0)}$. To determine the free energy per spin of the infinite system $f(K)$, which is the limit of $f(K,N)$ as N increases without bound, we take lim $N\to\infty$ followed by $m\to\infty$. Although the function g is analytic in the couplings, singularities in $f(K)$ can arise because the sum in Eq. (2.5) contains an infinite number of terms. For a finite system of N spins, the number of terms in the sum cannot exceed $\ln N/(d\ln b)$ so that the free energy $f(K,N)$ (being a finite sum of analytic functions) is analytic. It can be evaluated by iterating Eq. (2.5) to a value M chosen so that the number of spins $b^{-(M+1)d}N$ is small enough to permit the explicit calculation of $f(K^{(M+1)},b^{-(M+1)d}N)$, which is then inserted into Eq. (2.5). Because this equation so clearly demonstrates how the free energy of an infinite system grows out of that of finite systems it has been generally recognized that renormalization-group methods are particularly well suited to the calculation of finite size effects.[14] As renormalization-group transformation can rarely be carried out exactly it is necessary to employ an approximation scheme. In order to make manifest effects of finite size, such a scheme should reproduce the exact critical exponents in the infinite limit.

This program was first carried out by Berker and Ostlund.[7] They mapped the Hamiltonian of an adsorbed system onto a q-state Potts lattice gas and then they solved this model with an extremely simple Migdal approximation scheme. As all thermodynamic functions depended on the choice of q, this parameter could be adjusted to give the exact critical exponent of the infinite systems. The resulting "toy" recursion relations were completely adequate to demonstrate the effects of finite size. As noted by Berker and Ostlund, the price of the simplicity of the recursion relations is an alteration in the basic model solved. However as the evaluation of the thermodynamic functions of the original adsorbed systems, whether finite or infinite, was not their primary interest, this alteration was of little importance. In contrast, we require excellent approximations to the thermodynamic functions of the original model systems as we intend to compare our calculated functions with experiment in order to extract surface characterizations. We have chosen therefore to employ a different approximation scheme which we use on the ordinary lattice gas models of adsorption or their Ising model equivalents. Our method is lattice sensitive. We treat first the square lattice with nearest-neighbor interactions only.

A. Square lattice

The lattice of sites is divided into cells of four sites each in the usual way (Fig. 1) and the projection operator is taken to be a product of single-cell projection operators. Symmetry requires the single-cell projection operator to be of the form

$$P(S',S) = \tfrac{1}{2}+AS'(S_1S_2S_3+S_1S_2S_4+S_1S_3S_4+S_2S_3S_4) + BS'(S_1+S_2+S_3+S_4) , \quad (2.6)$$

where A and B are independent of the spins. We employ a two-cell approximation with periodic boundary conditions and the reduced Hamiltonian

$$\mathcal{H}_N = K\sum_{\langle ij\rangle} S_iS_j + H\sum_i S_i + NC ,$$

where $\langle ij\rangle$ denotes a sum over nearest-neighbor

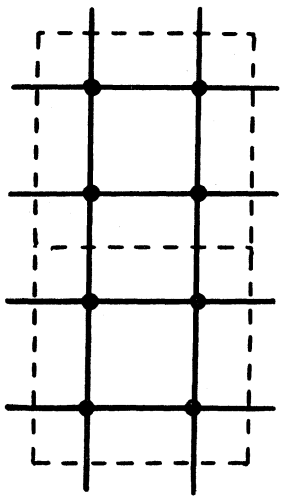

FIG. 1. A two-cell, eight-spin, periodically continued cluster for the square lattice.

pairs and N is the number of spins in the lattice. The recursion relations that result from Eqs. (2.1) and (2.6) are presented in Appendix A.

If we denote by V_3 and V_4 the values taken by P when S' equals $+1$ (denoted hereafter by "+") and three or four, respectively, of the S_i are +, then

$$A=(2V_4-4V_3+1)/16 \ , \tag{2.7}$$

$$B=(2V_4+4V_3-3)/16 \ . \tag{2.8}$$

The "majority rule" projection operator corresponds to choosing the values $V_3=V_4=1$. Although this simple projection operator works well at high and low temperatures, it does not yield the exact critical exponents in any approximation employing a few cells. We therefore adjust the values of V_3 and V_4 so as to reproduce the critical properties of the infinite system (in particular, the critical temperature and thermal eigenvalue), and then study the finite system results. The fitted values are found to be $\tilde{V}_3=1.0806$, and $\tilde{V}_4=1.0016$ which differ only slightly from majority rule values. The critical values and exponents for both majority rule and fitted values are shown in Table I. The weights V_3 and V_4 can be interpreted as the probability of the cell spin being + when three or four site spins, respectively, are +. Note that Eq. (2.6) requires V_2, the value of the single-cell projection operator, or "probability" of mapping to a + cell spin from two + site spins and two − spins to be identically equal to $\frac{1}{2}$. If each state in the partial partition function is to be summed with a positive weight, V_3 and V_4 must lie between zero and unity, consistent with their interpretation as probabilities. Note also that the "probability" that the cell spin is − when three or four site spins are + is $(1-V_3)$ or $(1-V_4)$, respectively.

The fact that $\tilde{V}_3$ and $\tilde{V}_4$ are greater than unity has little effect on the high-temperature ($K<K^*$) recursion relation, as in that limit all site spin configurations contribute equally. On the low-temperature ($K>K^*$) side, however, the recursion relation develops a singularity, as well as a spurious attractive fixed point with a complex (oscillatory) eigenvalue. Also, since the recursion relations with $V_4\neq 1$ fail to preserve the ferromagnetic ground state, $K'(K)$ is bounded, i.e., $K'<K'_{\max}$ (or $T>T_{\min}$). From Appendix A in the limit of large K,

$$K'_{\max}=\frac{1}{16}\ln\left[\frac{1+64(A+B)^2}{1-64(A+B)^2}\right]=\frac{1}{8}\ln\left[\frac{(V_4-\frac{1}{2})^2+\frac{1}{4}}{V_4(1-V_4)}\right] \ ,$$

which imposes a bound on $K'(K)$ if V_4 is not exactly zero or one. These values correspond to mapping four + site spins entirely to a − or + cell spin, respectively.

To circumvent these problems, V_3 and V_4 are allowed to depend on K. We choose them to differ from their majority rule values only in the neighborhood of the fixed point. In particular,

$$V_n(K)=1+(\tilde{V}_n-1)\exp[-(K-K^*)^2/2\sigma_K^2] \tag{2.9}$$

TABLE I. Critical values for square lattice.

A.	Majority rule $K^*\cong 0.6138$ $y_T\cong 0.6103$ $y_h\cong 1.961$	$(V_3=V_4=1)$
B.	Fitted values $K^*=\frac{1}{2}\ln(1+\sqrt{2})\cong 0.440\,68$ $y_T=1$ $y_h\cong 1.830$	$(V_3=\tilde{V}_3\cong 1.0806,\ V_4=\tilde{V}_4\cong 1.0016)$

for $n=3,4$. The recursion relations give the exact critical point and thermal eigenvalue, and deviate from majority rule values only in the critical region. The parameter σ_K is chosen to be 0.1 (by eye) to ensure that $K'(K)$ is smooth (see Fig. 2). For values of σ_K near 0.1, the thermodynamic functions calculated from the recursion relations are insensitive to the exact value of σ_K. The cluster we use (Fig. 1) has eight site spins and two cell spins; thus each iteration of our recursion relations reduces the degrees of freedom by a factor of 4. At the last step the free energy per spin of a periodically continued cluster of two spins is substituted into Eq. (2.5). Therefore after n iterations we are evaluating the free energy of a rectangular Ising system of 2^{2n+1} spins with periodically continued boundaries. The specific heat is obtained by iterating the first derivative of the free energy and numerically differentiating once.

Our results for the specific heat of rectangular periodic systems with 2^3, 2^5, 2^7, and 2^9 spins are displayed in Fig. 3(a). They are in qualitative agreement with the exact calculation of Ferdinand and Fisher[6] [Fig. 3(b)]. The peak shapes are quite similar and in both cases the peak temperatures are higher than the critical temperature. Although the systems considered in Fig. 3(b) are of different size and shape so no detailed quantitative comparison is possible, we compare in Fig. 3(c) the peak heights of systems with 2^m spins as calculated in Ref. 6 and by us. In Fig. 4, our result for an infinite system is compared with the exact Onsager[15] solution. The agreement is quite good, especially near the critical point.

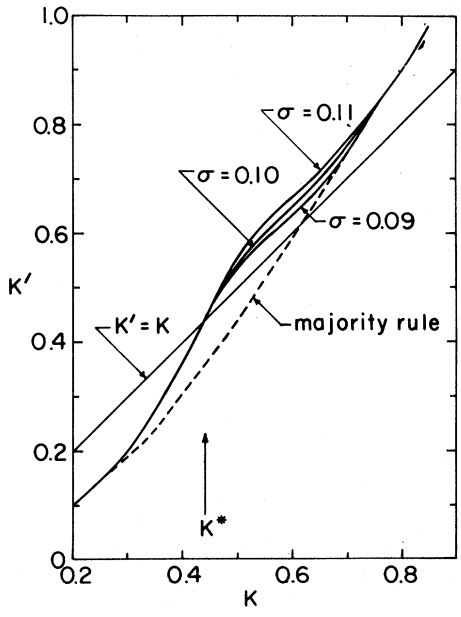

FIG. 2. The recursion relation for the square lattice. K' is plotted in solid lines as a function of K for $\sigma_K=0.09$, 0.10, and 0.11. In addition, the recursion relation for the majority rule is plotted as a broken line. The line $K'=K$ is also plotted to indicate the location of the fixed points.

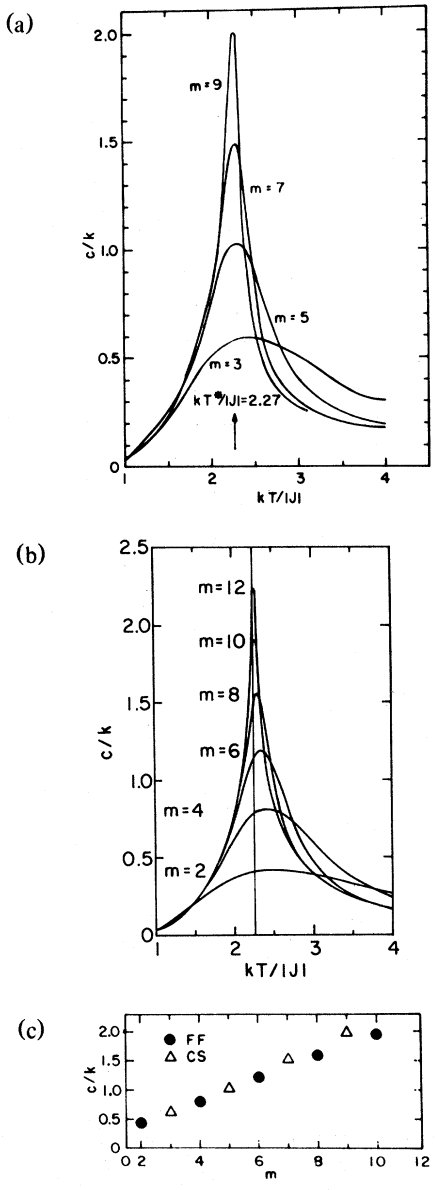

FIG. 3. (a) Specific heat of square lattice of 2^m spins, $m=3,5,7,9$, calculated approximately by the renormalization group as a function of $kT/|J|\equiv 1/|K|$. (b) Exact results of Ferdinand and Fisher for the specific heat of a square lattice of 2^m spins, with m taking several values. (c) Maximum specific heat of square lattice of 2^m spins. Circles—exact result of Ferdinand and Fisher; triangles—approximate results of this paper.

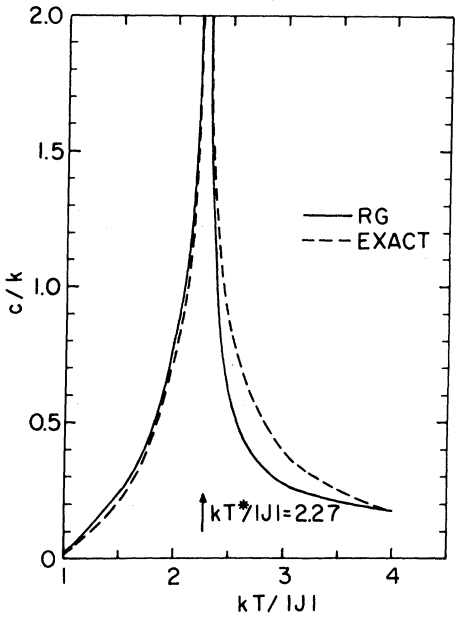

FIG. 4. Specific heat of an infinite square lattice calculated approximately by the renormalization group (solid lines) compared with the exact Onsager result (broken line). The exact critical temperature is indicated by an arrow.

B. Honeycomb lattice

We next consider the honeycomb lattice gas with repulsive nearest-neighbor interactions or its equivalent Ising model with antiferromagnetic interactions. The analysis is similar to that for the square lattice. A periodically continued cluster of two cells with four site spins each (Fig. 5) is used to generate the recursion relations. As with the square lattice, the projection operator is chosen to be a product of single-cell projection operators which is taken to be of the form

$$P(S',\{S\}) = \tfrac{1}{2} + AS'S_1S_2S_3 + BS'(S_1+S_2+S_3) \ , \tag{2.10}$$

where S_1, S_2, and S_3 are the spins on the perimeter of the cell. The critical temperature and exponents improve relative to exact values when, as in the above, the site spin in the center of the cell is omitted from the projection operator. The projection operator Eq. (2.10) preserves the symmetry of the two sublattices present in the site system, since the center spin on one cell belongs to the same sublattice as the three vertex spins in the other cell. This sublattice symmetry implies that the ferromagnetic ($K^* > 0$) and antiferromagnetic ($K^* < 0$) critical temperature and thermal eigenvalue are identical for zero applied magnetic field.

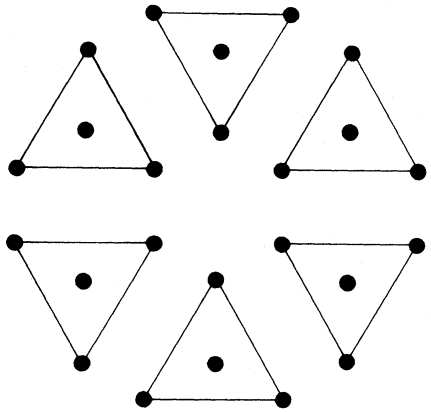

FIG. 5. Division of honeycomb lattice into cells.

If we denote by V_2 and V_3 the value of P when S' and two or three of the perimeter spins are $+$, then

$$A = -\tfrac{1}{4}(3V_2 - V_3 - 1) \ , \tag{2.11}$$

$$B = \tfrac{1}{4}(V_2 + V_3 - 1) \ . \tag{2.12}$$

The majority rule values are $V_2 = V_3 = 1$ and in this form the projection operator was used by Mahan and co-workers.[16] By analogy with our work on the square lattice, we can adjust V_2 and V_3 to fit the exact critical point ($K^* = 0.6585$) and thermal exponent ($y_T = 1$) for the infinite system. This fit requires $V_2 = \tilde{V}_2 \equiv 1.0438$ and $V_3 = \tilde{V}_3 = 1.0032$ at the critical point. The recursion relations for the honeycomb lattice are summarized in Appendix B, while the critical temperature and exponents for the majority rule[17] and fitted cases are listed in Table II. It should be noted that in the latter case the magnetic field in the antiferromagnet is irrelevant as expected.

Since V_2 and V_3 are greater than unity, the partial partition functions in the recursion relations involve sums over states weighted by a negative "probability." As was found for the square lattice, there appears an attractive fixed point with a complex eigenvalue at low temperatures, and $K'(K)$ is bounded. Since in this case the magnetic field is also included, there appears an additional problem—the partial partition function $Z(--)$ becomes negative for large positive H [while $Z(++)$ becomes negative for large negative H]. To remedy these difficulties, we choose

$$V_n(K,H) = 1 + (\tilde{V}_n - 1)\exp[-(K-K^*)^2/2\sigma_K^2 - H^2/2\sigma_H^2]$$

for $n = 2, 3$. As before, the value $\sigma_K = 0.1$ is chosen to make the recursion relations smooth. The value of σ_H is set to 1.0 (by eye) so the antiferromagnetic

TABLE II. Critical values for honeycomb lattice.

A.	Majority rule	$(V_2 = V_3 = 1)$
	Ferromagnetic	
	$K^* \cong 0.8490$	
	$y_T \cong 0.5545$	
	$y_h \cong 1.971$	
	Antiferromagnetic	
	$K^* \cong 0.8490$	
	$y_T \cong 0.5545$	
	$y_h \cong 0.9698$	
B.	Fitted Values	$(V_2 = \tilde{V}_2 \cong 1.0438,$
	Ferromagnetic	$V_3 = \tilde{V}_3 \cong 1.0032)$
	$K^* = \frac{1}{2}\ln(2+\sqrt{3}) \cong 0.6585$	
	$y_T = 1$	
	$y_h \cong 1.894$	
	Antiferromagnetic	
	$K^* = -\frac{1}{2}\ln(2+\sqrt{3}) \cong -0.6585$	
	$y_T = 1$	
	$y_h \cong -0.084\,54$	

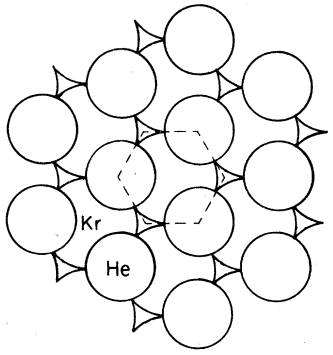

FIG. 7. Schematic of He-Kr-graphite adsorption. The krypton atoms (large circles) provide a honeycomb lattice for the helium atoms (small circles).

critical line is smooth (Fig. 6). The specific heat is relatively insensitive to the exact value of σ_H, provided it is near 1. Specific heats of finite systems of 2^{2n+1} spins (or 2^{2n} atoms in the He-Kr-graphite lattice gas, see Fig. 7) can be obtained as before. Instead of plotting the specific heat of the magnetic system at constant magnetization c/k as before, we present the heat capacity per atom at constant coverage C/Nk of the lattice gas where N is the number of atoms. These two quantities are related to

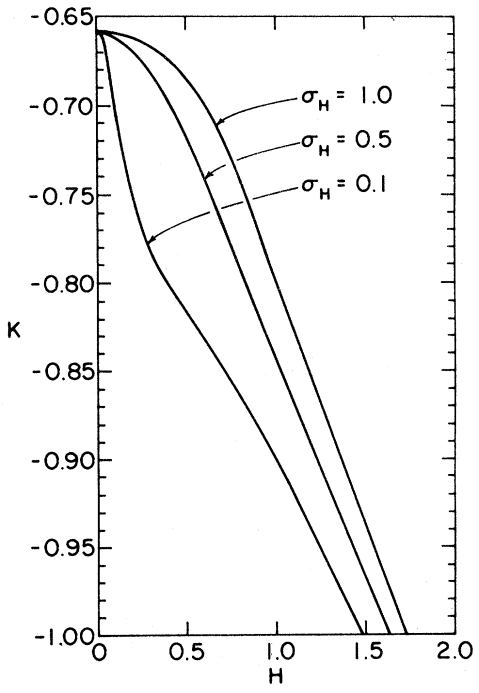

FIG. 6. Critical line for a honeycomb antiferromagnet. The critical line is plotted for $\sigma_H = 0.1$, 0.5, and 1.0.

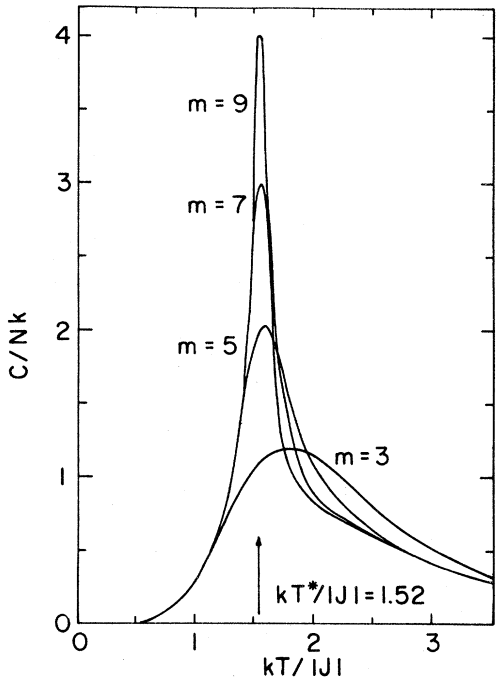

FIG. 8. Heat capacity per atom of honeycomb lattice gas of 2^m sites, $m = 3, 5, 7, 9$, and density $\frac{1}{2}$ calculated approximately by the renormalization group. Note that the peak temperatures are higher than the critical temperature, as in the case of the square lattice.

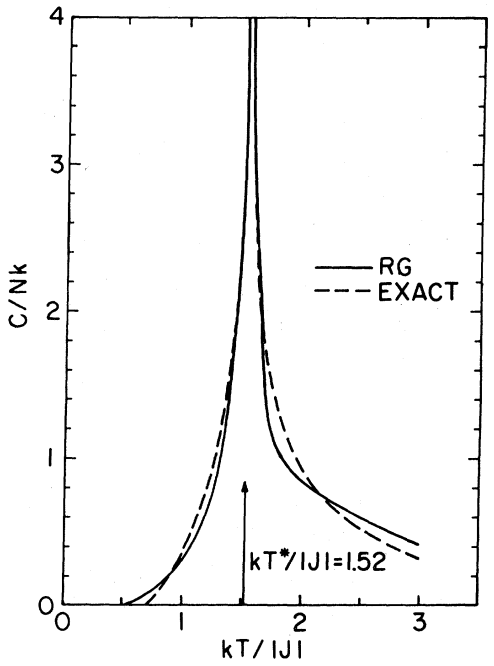

FIG. 9. Heat capacity per atom of an infinite honeycomb lattice gas at density $\frac{1}{2}$ calculated approximately by the renormalization group (solid line) compared to the exact Houtappel solution (broken line).

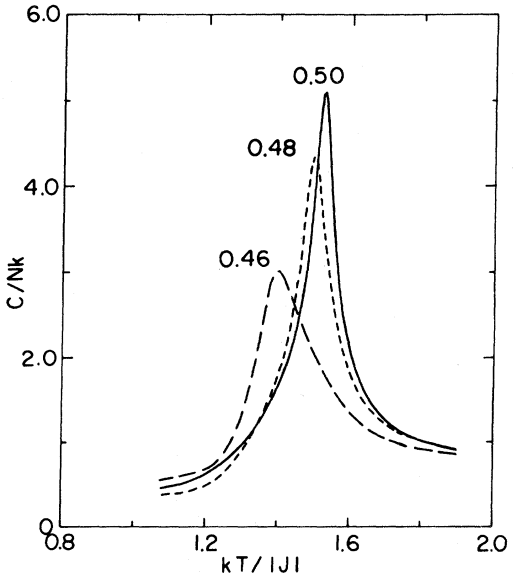

FIG. 10. Heat capacity per atom at various coverages for a system of 2^{11} adsorption sites.

one another according to $c/k = nC/Nk$. Figure 8 shows the heat capacity per atom at coverage $n = \frac{1}{2}$ for systems with 2^3, 2^5, 2^7, and 2^9 adsorption sites. The peak heights and shapes of the corresponding magnetic system are similar to those obtained for the square lattice and in both cases the peak temperature is higher than the critical temperature of the infinite systems. In Fig. 9 the infinite lattice gas result for $n = \frac{1}{2}$ is compared with the exact Houtappel[18] solution. The agreement is very good, especially near the critical point. In Fig. 10 we show the heat capacity per atom at constant coverage for several coverages in a system with 2^{11} adsorption sites. Note that the peaks become wider and more rounded as the coverage departs from $\frac{1}{2}$. This effect is more pronounced for larger systems.

III. EXTRACTION OF CHARACTERISTIC SUBSTRATE SIZES

Substrates used in adsorption experiments rarely consist of a single-crystal face but rather are composed of several facets or grains of varying sizes. Thus an experimental measurement arises from a composite of the responses of systems of different sizes. If the composite system contains $M(N_i)$ subsystems with N_i atoms each and a heat capacity per atom c_i, the specific heat of the composite C_{tot}/N is

$$C_{\text{tot}}/N = \sum_i M(N_i) N_i c_i \Big/ \sum_i M(N_i) N_i \equiv \sum_i \rho(N_i) c_i \ , \tag{3.1}$$

where $\rho(N_i)$ is the fraction of atoms in systems of size N_i and $N = \sum_i M(N_i) N_i$. As the specific heats c_i have been calculated at density $\frac{1}{2}$ for systems of size $N_i = 2^{2i}$, a distribution $\rho(N_i)$ can be inserted into the above and a specific heat predicted or, conversely, the experimental specific heat can be fitted and the distribution determined.

Before carrying out the latter, there are two additions to the above we shall make. First this expression assumes that all adsorbed atoms take part in the order-disorder transition. It makes no allowance for the possibility that some of the atoms are adsorbed on "hot spots" with large heats of adsorption (edges, steps, etc.) or are otherwise lost to the order-disorder process. As this appears to be likely, we include in the above a term denoted by $i = 0$ characterized by nonzero N_0 but $c_0 = 0$.

Second our lattice-gas specific heat contains no contribution from the kinetic energy, a contribution which is temperature dependent. We remedy this by fitting experimental data only in the vicinity of the transition temperature and adding to the above an analytic background $B_0 + B_1 T$. Thus we fit experi-

mental data to the form

$$\frac{C_{\text{tot}}}{N} = \sum_{i=0}^{I} \rho(N_i) c_i + B_0 + B_1 T \ . \tag{3.2}$$

Fitting parameters are I values of $\rho(N_i)$, B_0, and B_1. Clearly the precise values of $\rho(N_i)$ will be unreliable but we expect that certain characteristics of the resulting distribution will be stable with respect to variations in the value of I for example.

We employ such a procedure on the experimental data taken by Tejwani *et al.*[4] on the system He-Kr-graphite foam. For simplicity,[19] we assume their highest peak occurs at coverage $\frac{1}{2}$. To test the stability of the calculated distribution we use Eq. (3.2) with the largest system $N_I = 2^{2I}$ having $I = 6$, 8, and 10. The main features of the distribution are quite insensitive to these changes and the fit is excellent in all cases as might be expected (see Fig. 11). These features are as follows. First there is a large peak shared by $\rho(N_0)$ and $\rho(N_1)$, the fraction of atoms which do not contribute at all and the fraction in the smallest cluster of four atoms. As such a cluster can hardly be said to undergo a transition we lump these two together. Their sum is equal to 0.50. Thus of the total number of adsorbed atoms, 50% do not participate in the transition at all. Second, the distribution of the atoms which do undergo the transition is skewed with the largest fraction adsorbed on small platelets of the order of 100 Å but a small percentage adsorbed on sizes up to 1000 Å. (The size can be obtained from the N_i, the geometry of the honeycomb lattice and the fact that the lattice gas density is $\frac{1}{2}$.) If the 50% is ignored, the mean size of the adsorbing platelets is 140 Å with a standard deviation of 106 Å. The distribution with $I = 8$ is shown in Table III, and plotted in Fig. 12.

The error introduced by ignoring the contribution to the specific heat which scales as the perimeter can now be estimated. From finite size scaling[8] that part of the specific heat which scales as the area obtains a maximum $\sim L^2 \ln L$ while that which scales as the perimeter obtains a maximum $\sim L^2$. It is the sum of these two terms which should be related to the experimental maximum. Ignoring the contribution of the perimeter increases the estimate of the mean size by a factor $(1 + 1/\ln L)^{1/2}$. A mean size of 140 Å obtained above corresponds to $L \sim 40$ in units of the lattice spacing of the ordered array of helium atoms shown in Fig. 7. Thus the error in the mean of the distribution introduced by this approximation is of the order of 10% which is not very serious, particularly in light of a width of the distribution. Of course, the contribution of the perimeter is proportionally greater for smaller sizes so that including this contribution would tend to skew the distribution shown in Fig. 12 even more toward smaller sizes.

The result that 50% of the adsorbed atoms do not participate in the transition is consistent with that of Berker and Ostlund[7] who found that their calculated specific-heat values were much larger than those measured experimentally. They had assumed all atoms were adsorbed on platelets of the same size and all contributed to the signal. It can also be inferred from this result that the krypton preplating of the graphite foam is quite imperfect, affording preferred adsorption sites for much of the helium. Such a hypothesis is completely in accord with recent studies of the krypton-grafoil system[20] using extended x-ray fine structure. It was found that at 10 K and at

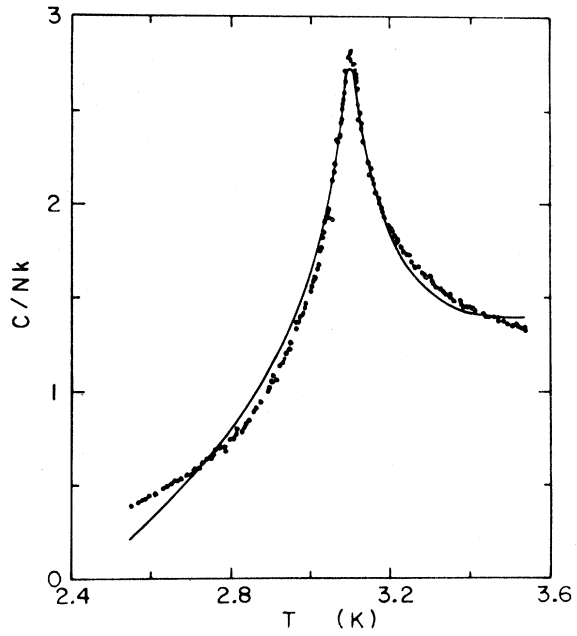

FIG. 11. Comparison of experimental data of Ref. 4 and best fit from Eq. (3.2).

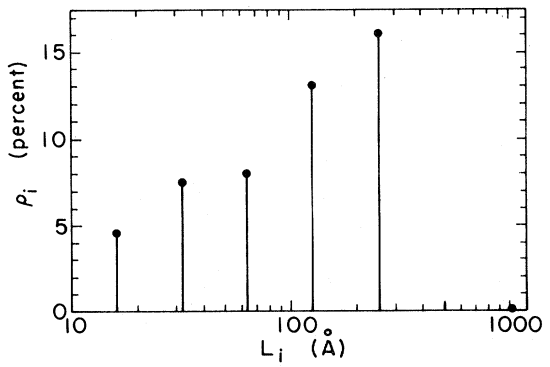

FIG. 12. Distribution $\rho(N)$ from Eq. (3.2), plotted as a function of characteristic length (defined to be the square root of the area) of each subsystem.

TABLE III. Fraction ρ_i of atoms adsorbed on areas of characteristic size L_i. See text for $i=0,+1$.

i	0+1	2	3	4	5	6	7	8
L_i(Å)		15.9	31.7	63.5	127	254	508	1016
ρ_i(%)	49.97	4.56	7.46	8.01	13.1	16.3	0.5	0.1

the low coverages studied (less than 0.35 of a krypton monolayer) most of the krypton did not form large uniform islands.

Our results for the characteristic size of krypton-plated graphite foam are the first for this system. The characteristic size of adsorption areas is typically determined from lineshapes obtained from diffraction experiments together with a substrate model which includes the effects of a single characteristic length and the distribution of orientations of the crystallites.[21] This combination of experiment and modeling yields characteristic sizes of the order of 100 Å for Grafoil,[21,22] and 450 Å for ZYX.[3] Thermodynamic measurements have also been combined with substrate models to obtain estimates of the characteristic size for Grafoil[12] of 100 Å and for graphite foam[23] an average domain radius of 600 Å. No results of either kind are available for Kr-plated foam.

We have shown that an alternative or perhaps supplementary procedure to determine characteristic sizes is to make use of the measured thermodynamic functions. This is possible because, as indicated, these functions of finite systems can be easily and reliably calculated.

ACKNOWLEDGMENTS

It is a pleasure to thank M. Barber, J. G. Dash, M. J. Tejwani, O. E. Vilches, and M. Wortis for many profitable discussions. This work was supported in part by National Science Foundation Grant No. DMR 79-20785.

APPENDIX A: RECURSION RELATIONS FOR SQUARE LATTICE

The partial partition functions $Z(S_1',S_2')$ are calculated by performing the sum Eq. (2.1) over all 256 site spin configurations. Thus,

$$Z(S_1',S_2') = \sum_{\{S\}} P(\{S\},\{S'\}) \exp H_N(K,\{S\}) \tag{A1a}$$

$$= \sum_{n=1}^{7} \left(\tfrac{1}{4}M_n + S_1'S_2'C_n\right) e^{E_nK} \tag{A1b}$$

$$\equiv \exp[4K'S_1'S_2' + H'(S_1'+S_2') + 2C'] \ , \tag{A1c}$$

where the M_n are the "multiplicities" or number of site spin configurations with energy E_nK. These coefficients are given in Table IV. The (renormalized) cell coupling constants are written in terms of the partial partition functions by using Eq. (A1c):

$$K' = \tfrac{1}{16} \ln\left[\frac{Z(++)Z(--)}{Z(+-)Z(-+)}\right] \ , \tag{A2a}$$

$$H' = \tfrac{1}{4} \ln\left[\frac{Z(++)}{Z(--)}\right] = 0 \ , \tag{A2b}$$

$$C' = \tfrac{1}{8} \ln[Z(++)Z(+-)Z(-+)Z(--)] \ , \tag{A2c}$$

where "+" and "−" are used for ± 1.

TABLE IV. Coefficients of recursion relations for square lattice.

n	M_n	C_n	E_n
1	2	0	−16
2	20	$-16(A-B)^2$	−8
3	48	$-32(A-B)^2-128B^2$	−4
4	116	$128A^2-32(A+B)^2$	0
5	48	$32(A-B)^2$	4
6	20	$16(A-B)^2+128(B^2-A^2)$	8
7	2	$32(A+B)^2$	16

with $A=(2V_4-4V_3+1)/16$
$B=(2V_4+4V_3-3)/16$

TABLE V. Coefficients of recursion relations for honeycomb lattice.

n	M_n	C_n	D_n	E_n
1	2	$-2(A+3B)^2$	0	-12
2	$16C_2$	$8(A^2-9B^2)\mathfrak{C}_2$	$12(A+B)\mathfrak{S}_2$	-6
3	30	$6(A+7B)(A-B)$	0	-4
4	$48C_2$	$24(B^2-A^2)\mathfrak{C}_2$	$-12(A-3B)\mathfrak{S}_2$	-2
5	$32(C_4+1)$	$8(\mathfrak{C}_4-1)(A^2+3B^2)$	$8(A+6B)\mathfrak{S}_4$	0
6	$48C_2$	$-24(B^2-A^2)\mathfrak{C}_2$	$-12(A-3B)\mathfrak{S}_2$	2
7	$6(1+4C_4)$	$-6(A-B+8B\mathfrak{C}_4)(A-B)$	$-12(A-3B)\mathfrak{S}_4$	4
8	$16C_6$	$-8(A^2-9B^2)\mathfrak{C}_6$	$4(A+9B)\mathfrak{S}_6$	6
9	$2C_8$	$2(A+3B)^2\mathfrak{C}_8$	$2(A+3B)\mathfrak{S}_8$	12

$\mathfrak{C}_n \equiv \cosh(nH)$ $\quad \mathfrak{S}_n \equiv \sinh(nH)$

$A-B=\frac{1}{2}(1-2V_2)$
$A+B=\frac{1}{2}(V_3-V_2)$
$A+3B=\frac{1}{2}(2V_3-1)$

APPENDIX B: RECURSION RELATIONS FOR HONEYCOMB LATTICE

The partial partition functions for the honeycomb lattice can be expressed in the form

$$Z(S_1',S_2') = \sum_{n=1}^{9} [\tfrac{1}{4}M_n(H) + \tfrac{1}{2}D_n(H)(S_1'+S_2') + C_n(H)S_1'S_2']e^{E_nK}$$
$$\equiv \exp[3K'S_1'S_2' + H'(S_1'+S_2') + 2C'] \ , \tag{B1}$$

where the coefficients M_n, D_n, and C_n are given in Table V. The renormalized couplings are then given by

$$K' = \tfrac{1}{12}\ln\left[\frac{Z(++)Z(--)}{Z(+-)Z(-+)}\right] \ , \quad H' = \tfrac{1}{4}\ln\left[\frac{Z(++)}{Z(--)}\right] \ , \quad C' = \tfrac{1}{8}\ln[Z(++)Z(+-)Z(-+)Z(--)] \ . \tag{B2}$$

[1]M. Bretz and J. G. Dash, Phys. Rev. Lett. 27, 647 (1971).
[2]M. Bretz, Phys. Rev. Lett. 38, 501 (1977).
[3]P. M. Horn, R. J. Birgeneau, P. Heiney, and E. M. Hammonds, Phys. Rev. Lett. 41, 961 (1978).
[4]M. J. Tejwani, O. Ferreira, and O. E. Vilches, Phys. Rev. Lett. 44, 152 (1980); M. J. Tejwani, dissertation (University of Washington, 1979) (unpublished).
[5]R. L. Park, T. L. Einstein, A. R. Kortan, and L. D. Roelofs, in *Ordering in Two Dimensions,* edited by S. K. Sinha (North-Holland, New York, 1980).
[6]A. E. Ferdinand and M. E. Fisher, Phys. Rev. 185, 832 (1969); M. E. Fisher and A. E. Ferdinand, Phys. Rev. Lett. 19, 169 (1967).
[7]A. N. Berker and S. Ostlund, J. Phys. C 12, 4961 (1979).
[8]M. E. Fisher and M. N. Barber, Phys. Rev. Lett. 28, 1516 (1972).
[9]See, for example, N. M. Svrakic and M. Wortis, Phys. Rev. B 15, 396 (1977).
[10]S. Ostlund and A. N. Berker, Phys. Rev. Lett. 42, 843 (1979).
[11]A. F. Silva-Moreira, J. Codona, and D. L. Goodstein, Phys. Lett. 76A, 324 (1980).
[12]T. T. Chung and J. G. Dash, Surf. Sci. 66, 559 (1977).
[13]An excellent review of position-space renormalization-group methods is Th. Niemeijer and J. M. J. van Leeuwen, in *Phase Transitions and Critical Phenomena,* edited by C. Domb and M. S. Green (Academic, London, 1976), Vol. 6.
[14]Such a program appears, for example, in B. Nienhuis, dissertation (Rijksuniversiteit Utrecht, 1978) (unpublished).
[15]L. Onsager, Phys. Rev. 65, 117 (1944).
[16]K. R. Subbaswamy and G. D. Mahan, Phys. Rev. Lett. 37, 642 (1976); G. D. Mahan and F. H. Claro, Phys. Rev. B 16, 1168 (1977).
[17]Our results for the exponents and critical temperature for the majority rule case differ from those of Subbaswamy and Mahan, Ref. 16.
[18]R. M. F. Houtappel, Physica (Utrecht) 16, 425 (1950).
[19]While the heat capacity per unit area has its peak at density $\frac{1}{2}$, the heat capacity per particle does not. This effect is negligible here.
[20]C. Bouldin and E. A. Stern (unpublished).
[21]J. K. Kjems, L. Passell, H. Taub, J. G. Dash, and A. D. Novaco, Phys. Rev. B 13, 1446 (1976).
[22]K. Carneiro, J. Phys. (Paris) 38, C4-1 (1977).
[23]M. Bienfait, J. G. Dash, and J. Stoltenberg, Phys. Rev. B 21, 2765 (1980).